

Chaotic Behavior in Nonlinear Hamiltonian Systems and Equilibrium Statistical Mechanics

Roberto Livi,¹ Marco Pettini,² Stefano Ruffo,¹ and Angelo Vulpiani³

Received March 13, 1987

The relation between chaotic dynamics of nonlinear Hamiltonian systems and equilibrium statistical mechanics in its canonical ensemble formulation has been investigated for two different nonlinear Hamiltonian systems. We have compared time averages obtained by means of numerical simulations of molecular dynamics type with analytically computed ensemble averages. The numerical simulation of the dynamic counterpart of the canonical ensemble is obtained by considering the behavior of a small part of a given system, described by a microcanonical ensemble, in order to have fluctuations of the energy of the subsystem. The results for the Fermi–Pasta–Ulam model (i.e., a one-dimensional anharmonic solid) show a substantial agreement between time and ensemble averages independent of the degree of stochasticity of the dynamics. On the other hand, a very different behavior is observed for a chain of weakly coupled rotators, where linear exchange effects are absent. In the high-temperature limit (weak coupling) we have a strong disagreement between time and ensemble averages for the specific heat even if the dynamics is chaotic. This behavior is related to the presence of spatially localized chaos, which prevents the complete filling of the accessible phase space of the system. Localized chaos is detected by the distribution of all the characteristic Liapunov exponents.

KEY WORDS: Ergodic property; ensembles; deterministic chaos; numerical experiments; Liapunov exponents.

¹ Dipartimento di Fisica, Università degli Studi di Firenze, and Istituto Nazionale di Fisica Nucleare, Sezione di Firenze, 50125 Firenze, Italy.

² Osservatorio Astrofisico di Arcetri, and Istituto Nazionale di Fisica Nucleare, Sezione di Firenze, 50125 Firenze, Italy.

³ Dipartimento di Fisica, Università di Roma I, and Gruppo Nazionale Struttura della Materia-Centro Interuniversitario di Struttura della Materia, Sezione di Roma, 00185 Rome, Italy.

1. INTRODUCTION

There exist different approaches to the interpretation of the statistical description of a macroscopic object. One is based on the introduction of statistical ensembles and stresses the probabilistic aspects. Another underlines the importance of dynamics and it is founded on time averages resulting from the dynamical evolution. These two approaches are equivalent if the ergodic hypothesis is valid.

However, there exists no proof of ergodicity of a generic system; and the relation between these different approaches is still unclear.

There is a widespread attitude that considers the ensemble approach as the only significant one.⁽¹⁾ Some authors, although they have explicitly taken into account the relevance of dynamics, have reached the conclusion that the two quoted approaches are equivalent as far as the physical consequences are concerned. For instance, Khinchin⁽²⁾ and Truesdell⁽³⁾ suggest, on the basis of some probability theorems, that for the “relevant” observables, time averages and ensemble averages should coincide, independent of ergodicity. On the other hand, Chirikov and co-workers⁽⁴⁾ argue that for particular systems the ergodic hypothesis could be valid in the thermodynamic limit.

More recent results^(5,6) show that these statements are far from conclusive. For instance, in a chain of nonlinearly coupled oscillators equipartition of energy is violated if the energy density is smaller than a critical value, independent of the number of degree of freedom N .⁽⁶⁾ For some particular systems one can also obtain analytical bounds independent of N .⁽⁷⁾

Moreover, it is well known that integrable systems may not have the expected statistical behavior. For instance, this is the case of the Fourier law of heat conduction. Since the pioneering work by Schrödinger,⁽⁸⁾ it has been shown that a harmonic system interacting with two heat baths at different temperatures does not follow the phenomenological law; only those systems having suitable chaotic properties are in agreement with the phenomenology.⁽⁹⁾

Anyway, in such work on heat conduction, deterministic behavior—due to the dynamics—and stochastic effects—due to the presence of the heat baths—coexist. As a consequence, the actual role played by the dynamics in determining the statistical properties of the model is not clear.

In this paper we study the effect of ergodicity-breaking on equilibrium statistical mechanics for two different Hamiltonian models. Some preliminary results can be found in Ref. 10. Here we consider a model of nonlinearly coupled oscillators, the Fermi–Pasta–Ulam (FPU) model,⁽¹¹⁾ and a system of coupled rotators.

The canonical ensemble averages over suitable observables (giving thermodynamic quantities such as the specific heat) are compared with the corresponding time averages computed numerically along the “trajectories” of the systems. In numerical experiments, following the standard textbook definition, we simulate the canonical ensemble, considering a small part of a conservative system; in such a way we avoid the introduction of a noise source modeling the heat bath.

In order to make an unambiguous comparison between time and ensemble averages we had to choose an ensemble such that some physical quantities could be analytically computable. The canonical ensemble is fit for this purpose; in fact, computing averages with, for instance, the microcanonical ensemble would be a very hard task. The details of these models and the numerical method used in this work are discussed in Section 2. Section 3 is devoted to a comparison between ensemble and time averages.

With regard to the FPU model, a qualitative agreement seems to hold. This could suggest the validity of Khinchin’s approach, although a small but systematic deviation of the dynamical result with respect to the ensemble prediction is present. This point will be discussed in Section 3.

We have obtained a significantly different scenario for the model of coupled rotators. In this case, at low temperatures we observe an agreement between time and ensemble averages. In contrast, in the high-temperature region we obtain an unexpected behavior: although the maximum Liapunov characteristic exponent is positive (i.e., the system is chaotic), there is a marked difference between time and ensemble averages in the specific heat.

In Section 4 we interpret this peculiar behavior in terms of “localized” chaos, i.e., the trajectories seem to span only subsets of the whole phase space.

Conclusions are presented in Section 5.

2. THE DYNAMICAL MODELS

In the present work we consider dynamical systems composed of N nonlinearly coupled particles with nearest-neighbor interaction described by the Hamiltonian

$$H = \sum_{i=1}^N \left[\frac{1}{2} p_i^2 + V(q_{i+1} - q_i) \right] \quad (1)$$

and with periodic boundary conditions, i.e., $q_{N+1} = q_1$.

We consider two dynamical models according to the following choices of the interaction potential. In the first model (FPU) we have⁽¹¹⁾

$$V(\xi) = \frac{1}{2} \xi^2 + \frac{1}{4} \lambda \xi^4 \quad (2)$$

The canonical coordinates q_j and p_j are the displacements from the equilibrium positions of nearest neighbor masses coupled by nonlinear springs in a one-dimensional lattice and the conjugate momenta, respectively. In the second model we have

$$V(\xi) = \varepsilon(1 - \cos \xi) \quad (3)$$

The canonical coordinates q_j and p_j are the angular coordinates and the angular momenta, respectively, of a chain of N rotators. In the limit $\varepsilon \rightarrow 0$ model (3) is already in action-angle coordinates, and the frequencies $\omega_i(p_i) = (\partial H / \partial p_i) = p_i$ coincide with the action variables.

The Hamiltonian of this system is a prototype for spin systems of statistical mechanics.

We have integrated the equations of motion derived from these Hamiltonians in the following form

$$\ddot{q}_i = -\frac{\partial V}{\partial q_i} = F_i(\mathbf{q}) \quad (4)$$

by means of a standard leapfrog algorithm⁽¹²⁾

$$q_i(t + \Delta t) = 2q_i(t) - q_i(t - \Delta t) + (\Delta t)^2 F_i\{\mathbf{q}(t)\} \quad (5)$$

This is a canonical integration scheme, which does not alter the symplectic structure of our Hamiltonian systems; the errors are of order $(\Delta t)^4$ and with a suitable choice of the integration time step we obtain an excellent conservation of total energy E with zero mean fluctuations around the average value and relative errors $\Delta E/E$ ranging from 10^{-5} to 10^{-6} .

The simulation technique of the dynamics of a canonical ensemble consists in subdividing a chain of N particles into n subsystems of m particles each, $N = nm$. Passing from the microcanonical to the canonical ensemble, we should have: (a) $E_i \ll E$, i.e., the energy of the i th subsystem must be much smaller than the total energy, which amounts to having n large; (b) m large (thermodynamic limit), which leads to negligible average interaction energy between the subsystem and the remaining part of the original microcanonical system, which acts as a heat bath.

In our numerical simulations we have used typically $E_i \simeq 10^{-2} E$. In

previous work^(6,13) we have shown that a reasonable “simulacre” of the thermodynamic limit properties of such systems can be obtained by choosing m not extremely large. Moreover, the ratio between the average interaction energy and the total energy of a subsystem can be *a priori* estimated as $O(1/m)$.

Together with the dynamics $(\mathbf{p}(t), \mathbf{q}(t))$ of the models under consideration we can follow the time evolution of any function $f(\mathbf{p}, \mathbf{q})$.

Let us consider a given function of the coordinates of a system; we label f_j such a function for the j th subsystem. We have $f_j = f_j(\{p_i\}; \{q_i\})$ with $i \in [m(j-1) + 1, mj]$. Then we define the time average over a time \mathcal{T} of a physical quantity as follows:

$$\bar{f}^{\mathcal{T}} = \frac{1}{n} \sum_{j=1}^n \frac{1}{\mathcal{T}} \int_0^{\mathcal{T}} dt f_j[\{p_i(t)\}, \{q_i(t)\}] \tag{6}$$

The additional averaging over all the subsystems has been introduced because there is no reason to privilege one subsystem, and this improves the statistics. When $\mathcal{T} \rightarrow \infty$ we have $\bar{f}^{\mathcal{T}} \rightarrow \bar{f}$, using \bar{f} to represent the asymptotic time average. We shall replace such asymptotic averages with finite-time averages whenever a good convergence is found.

In the present paper we are dealing with time averages (6) and ensemble averages of potential energy and of specific heat. We have

$$\bar{\mathcal{U}} = \lim_{\mathcal{T} \rightarrow \infty} \frac{1}{n} \sum_{j=1}^n \frac{1}{\mathcal{T}} \int_0^{\mathcal{T}} dt \left\{ \sum_{i=m(j-1)+1}^{mj} V(q_{i+1}(t) - q_i(t)) \right\} \tag{7}$$

for the time average of potential energy; in curly brackets there is \mathcal{U}_j .

Following the standard definition of specific heat at constant volume, one has

$$\bar{C}_V = (\bar{E}_j^2 - \bar{E}_j^2)/mT^2 \tag{8}$$

where the following natural definition for the temperature has been adopted:

$$\frac{1}{2} T = \lim_{\mathcal{T} \rightarrow \infty} \frac{1}{N} \sum_{i=1}^N \frac{1}{\mathcal{T}} \int_0^{\mathcal{T}} dt \frac{1}{2} p_i^2(t) \tag{9}$$

and the energy of the j th subsystem is given by

$$E_j = \sum_{i=m(j-1)+1}^{mj} \left[\frac{1}{2} p_i^2 + V(q_{i+1} - q_i) \right] \tag{10}$$

The definition of temperature in Eq. (9) may appear arbitrary. Usually temperature is defined by means of ensemble theory; but here we deal with time averages and the definition (9) seems the natural one. We remark that this choice leads to equivalence of time and ensemble averages at least for kinetic energy.

We have always chosen random initial conditions; the details will be given for each model in subsequent sections.

Not only thermodynamic quantities have been measured, like \bar{u} and \tilde{C}_v , but also dynamical indicators of chaoticity of the phase space trajectories. We have computed all the Liapunov characteristic exponents (LCE) for these systems using the standard method,⁽¹⁴⁾ whose details are sketched in Appendix A.

3. COMPARISON BETWEEN TIME AND ENSEMBLE AVERAGES

3.1. The FPU model

In this section we report the numerical results obtained for the FPU model, Eq. (2), with the choice $\lambda = 0.1$; these results give us the time averages of some observables, which have to be compared with their corresponding ensemble averages (computed in Appendix B).

We have used $n = m = 32$. This choice of the parameters is a good compromise between a meaningful physical approximation and the feasibility of simulation for computer time requirements. In fact, we know that when the number of degrees of freedom is of the order of 20, a reasonable convergence to the “thermodynamic limit” is already obtained. This is observed when studying the relaxation toward equilibrium and non-equilibrium stationary states⁽⁶⁾ and the distribution of Liapunov characteristic exponents.⁽¹³⁾ The curves of the spectral entropy versus the energy density in the first case and the curves representing the distributions of LCE are found to superpose independent of the value of the number of degrees of freedom m in a wide range of values, provided that $m \gtrsim 20$. As far as n is concerned, we have estimated that $n = 32$ is reasonable after having examined the n and m dependences of our results.

As we want to measure the energy fluctuations due to the dynamics, the time integration steps have been varied (according to the different values of the total energy of the system) in order to reduce as much as possible the level of numerical noise. So we have used Δt ranging from 0.03 to 0.003, thus obtaining relative fluctuations of the total energy of $O(10^{-6})$.

The choice of initial conditions for the numerical simulations cannot be completely arbitrary, because we have chosen to compare time averages

with canonical ensemble averages. In fact, when using the canonical ensemble all the possible states in phase space are taken into account with the Gibbs weight; thus, the dynamical evolutions originating from initial conditions of low probability with respect to this measure could be exceptional paths in phase space. As we deal with a finite number of degrees of freedom, the canonical measure is not strictly orthogonal to other measures in phase space, such as Lebesgue measure, but in practice different choices of initial conditions (e.g., those of Ref. 6) would raise the problem of knowing if such paths could eventually join regions of larger measure during observation time scales.

As a consequence of the above considerations, we have taken as initial conditions

$$\begin{aligned}
 p_i(0) &= 0 \\
 q_i(0) &= \sum_{j=1}^{N/2} A_j \cos\left(\frac{2\pi j i}{N} + \psi_j\right) \\
 A_j &= a/j
 \end{aligned}
 \tag{11}$$

where ψ_j are random phases uniformly distributed in the interval $[0, 2\pi]$. This means that at $t=0$ the spatial Fourier spectrum of $\{q_i\}$ is $|\tilde{q}(k_n)|^2 \approx k_n^{-2}$. These random initial conditions belong to the support of the Gibbs canonical measure; in fact, as the p_i are Gaussian variables with

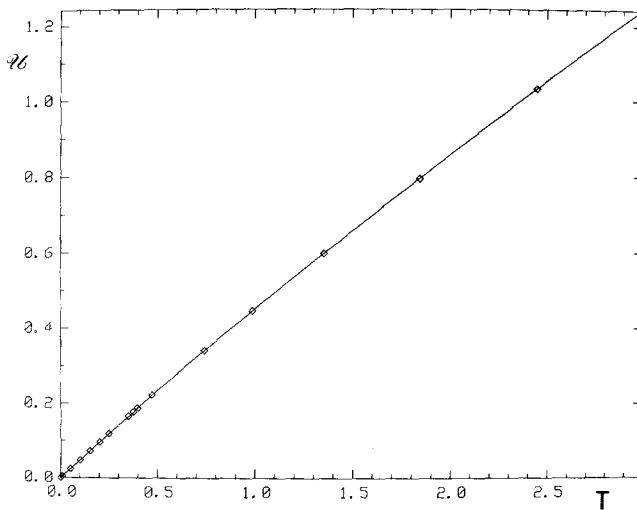


Fig. 1. Average potential energy versus temperature in the FPU model. (—) $\langle \mathcal{U} \rangle$ given by (B.11) and (B.12). (\diamond) Time averages.

zero mean setting, $p_i(0)=0$ means that the most probable values of the p_i are taken; moreover, the choice of the q_i as in Eq. (11) introduces an average property (energy equipartition among normal modes) in a single configuration. Another way of generating initial conditions belonging to the support of the canonical measure is to use a Monte Carlo technique with the Hamiltonian in Eq. (2). Some tests have been performed also with initial conditions generated by a Monte Carlo program; the subsequent dynamical behavior gave statistical results in perfect agreement with the previous ones.

The existence of a violation of equipartition at low energy densities⁽⁶⁾ implies the nonergodicity of the Hamiltonian flux in phase space; hence, it is a natural development to investigate the effects of ergodicity-breaking on the thermodynamic properties of this system. We have measured the average specific potential energy $\bar{\mathcal{U}}$, the specific heat \tilde{C}_V , and the maximal Liapunov exponent as given by Eqs. (7), (8), and (A.3) as functions of the temperature. The $\langle \mathcal{U} \rangle$ and C_V are also given by Eqs. (B.12) and (B.7), respectively, as ensemble averages. We performed the numerical integrations up to times $t_{\max} \simeq 5 \times 10^4$ (from $\sim 2 \times 10^6$ up to $\sim 2 \times 10^7$ integration steps) and we always had a good convergence to the asymptotic values of $\bar{\mathcal{U}}$ and \tilde{C}_V . The comparisons are reported in Figs. 1 and 2, respectively. Figure 1 shows an impressive excellent agreement between the two

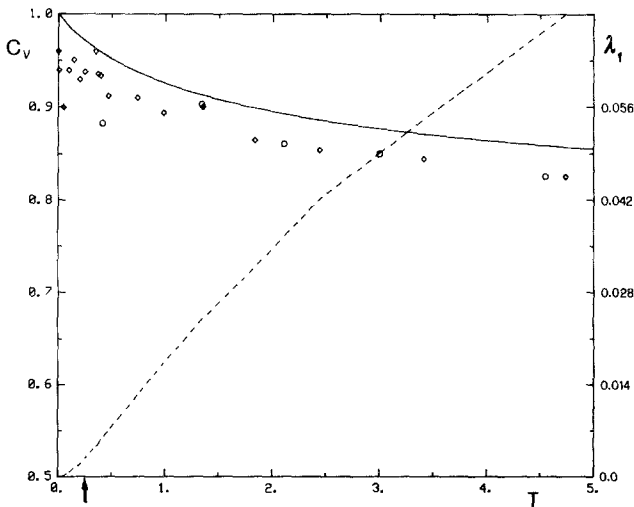


Fig. 2. Specific heat versus temperature in the FPU model. (—) C_V given by (B.7) and (B.9). (\square) \tilde{C}_V obtained with initial conditions at equipartition. (\circ) Nonequilibrium initial conditions. (---) The maximal Liapunov exponent λ_1 (the scale for λ_1 is on the right side). The arrow at the bottom indicates the equipartition threshold value.

kinds of averages. We have here a direct confirmation of the reliability of our numerical simulations of canonical ensemble. On the other hand, this result is not *a priori* obvious, as we shall see for the case of coupled rotators.

Figure 2 displays a qualitative agreement between \tilde{C}_V and C_V . Anyway the experimental data are systematically displaced toward slightly smaller values, the deviation is about 3% on the average. However, denoting by ϵ_c the critical energy density of the equipartition threshold of Ref. 6 (this threshold corresponds to a temperature $T_{th} = \epsilon_c$), we stress that, surprisingly, no significant change shows up in the behavior of specific heat—or potential energy—when the temperature passes through the threshold value T_{th} . We shall comment in the following about this point.

3.2. The Coupled Rotators Model

In this section we report the results obtained for the model described by the Hamiltonian (3) with the choice $\epsilon = 0.05$.

Let us remark that this system has two integrable limits for a fixed value of the coupling constant: (a) for vanishing energy one has a har-

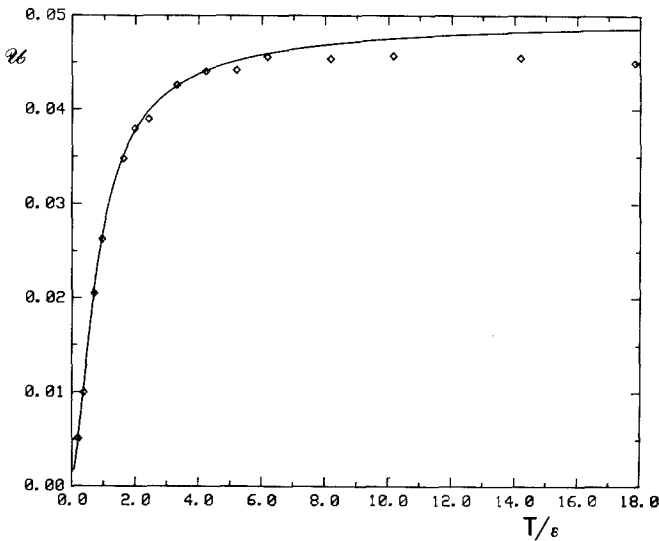


Fig. 3. Average potential energy versus temperature in the rotator model. (—) $\langle U \rangle$ given by (B.19). (\diamond) Time averages. The temperature is expressed in units of the coupling constant.

monic chain of oscillators, (b) at infinite energy, because of the boundedness of the potential, a system of independent rotators is left.

We have adopted $n = m = 10$ and $n = m = 20$. These values are slightly smaller than the previous ones used for the FPU model only for practical reasons (computing trigonometric functions requires a larger amount of CPU time with respect to algebraic powers). Nevertheless, as far as the thermodynamic limit problem is concerned, these values are already in the good range.

Again we have chosen random initial conditions in the form

$$q_i(0) = 0, \quad p_i(0) = B\alpha_i \quad (12)$$

where α_i is a random number uniformly distributed in the interval $[-1, 1]$ or with a Gaussian distribution with zero mean and variance equal to one; the value of B is given by the chosen value of temperature. We also used random $q_i(0)$ in order to check the sensitivity of the results on the initial conditions.

In Fig. 3 we compare $\bar{\mathcal{U}}$ and $\langle \mathcal{U} \rangle$ at different temperatures, and Fig. 4 we compare \tilde{C}_V and C_V together with λ_1 .

For the potential energy we observe a very good agreement between time and ensemble averages; only at high temperatures does a systematic small deviation show up. This can be understood with the following

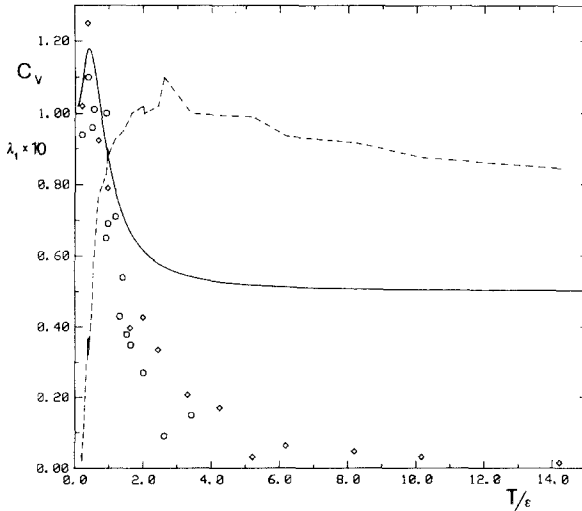


Fig. 4. Specific heat versus temperature in the rotator model. (—) C_V given by (B.17). (\circ) Ten subsystems of ten rotators. (\diamond) Twenty subsystems of twenty rotators. (---) λ_1 (the scale on the left gives $10\lambda_1$). The temperature is expressed in units of the coupling constant.

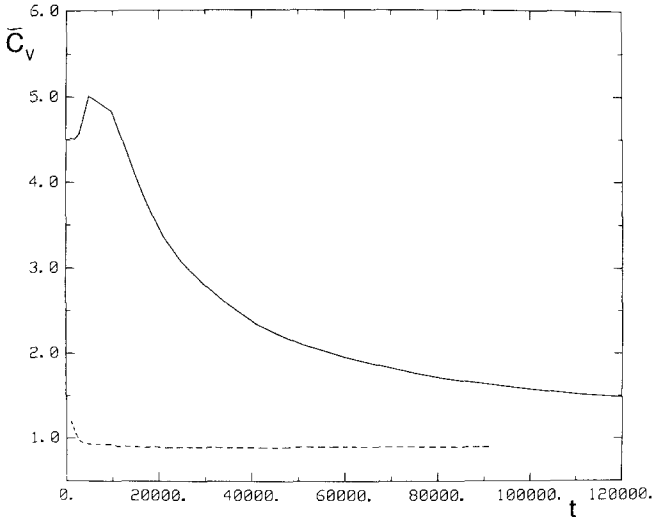


Fig. 5. Probability distribution $P(\mathcal{E})$ versus the normalized energy \mathcal{E} of a subsystem in the rotator model at different temperatures: (a) $T/\varepsilon = 1.0$, (b) $T/\varepsilon = 10$, (c) $T/\varepsilon = 20$.

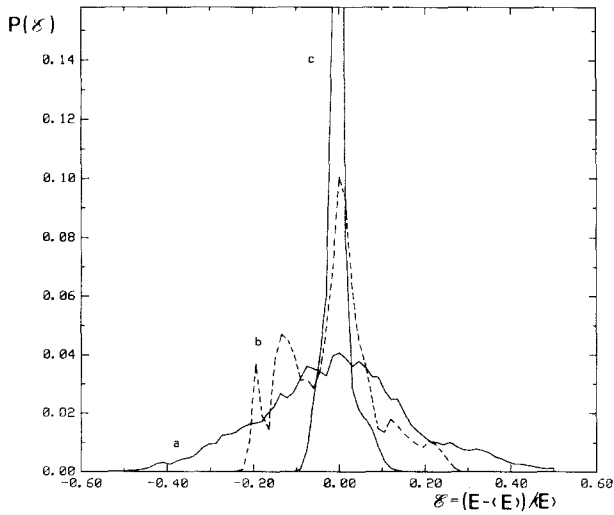


Fig. 6. Specific heat \tilde{C}_V versus time in the FPU model. Nonequilibrium initial conditions were assumed with (—) $T = 0.176 < T_c$ or (---) $T = 1.13 > T_c$. Slow relaxation below the equipartition threshold is evident.

argument. In the limit of $T \rightarrow \infty$, the ensemble average corresponds to considering the coordinate $(q_{i+1} - q_i)$ uniformly distributed between 0 and 2π and this gives $\langle \mathcal{U} \rangle = \varepsilon$. From the positive value of λ_1 we can infer that there are some residual correlations among the q_i and these are at the origin of the small observed differences between $\bar{\mathcal{U}}$ and $\langle \mathcal{U} \rangle$.

As for the specific heat (Fig. 4), we observe an agreement at low temperatures independent of the value of λ_1 . This situation is not surprising, because at small energy the system of rotators is essentially a chain of oscillators with a weak nonlinear coupling, similar to the FPU model. Increasing the temperature, \tilde{C}_V drops to very small values, in strong disagreement with C_V . We want to stress that this happens in a chaotic situation (λ_1 positive). We return to this apparently paradoxical behavior in the next section.

A direct method of visualizing the fluctuation of the energy E_j of a subsystem also has been adopted. Histograms of E_j at different temperatures have been constructed (Fig. 5); in the figure the index j is omitted. We remark that at intermediate temperature the distribution $P(\mathcal{E})$ is qualitatively a Gaussian with the right spread given by \tilde{C}_V , while, when the temperature is increased, $P(\mathcal{E})$ becomes strongly peaked around the average value (so \tilde{C}_V is very small).

4. DISCUSSION

For the FPU model, the observed qualitative agreement between time and ensemble averages—independent of the chaoticity—could be interpreted as a confirmation of the Khinchin–Truesdell approach. According to this point of view, for relevant physical observables the ergodic hypothesis should be the consequence of the great number of degrees of freedom rather than of the chaotic behavior of the system. However, we note that the normal modes are the “good” coordinates that are decoupled when the energy vanishes; in contrast to “real space” coordinates, the subsystems can also exchange energy only through linear coupling. Nevertheless, there is no contradiction with the failure of energy equipartition found in previous work⁽⁶⁾; indeed, this phenomenon is detected looking at a quantity related to normal modes.

More generally, from a physical point of view the relevant question regards the existence of an ergodicity restricted to a given function; therefore, it is possible that for a given system some functions display ergodicity, while others do not.

One can wonder what would happen with different initial conditions. We have assumed initial conditions that are presumably far outside the support of the Gibbs measure, like wave packets. The first four normal

modes of each subsystem have been excited with equal amplitudes and at different energies. The results so obtained show the following behavior: (a) For $T > T_{th}$ the values of \tilde{C}_ν are in good agreement with the previous ones; (b) when $T < T_{th}$ we observe very slow relaxations starting very far from the values given by the ensemble averages (Fig. 6). Apparently the temperature is lower, the slower are the relaxations. Unfortunately, detecting these phenomena is a heavy task because of computer time requirements, and a systematic investigation of this point is omitted. These results suggest that the existence of the equipartition threshold is a relevant fact only for nonequilibrium properties.

The situation looks more intricate in the case of rotators. At high temperatures, in spite of the exponential divergence of nearby trajectories in phase space ($\lambda_1 > 0$) the energy exchange among the subsystems is very small. This demonstrates the inconsistency of the naive idea that chaoticity implies good statistical properties. One can imagine that even though the trajectories are chaotic, they do not span uniformly the accessible phase space, but they are rather confined in some subregion. A way to infer something about this point consists in measuring all the Liapunov exponents $\{\lambda_i\}$, which are reported in Fig. 7 for $N = 20$ and random initial conditions.

There is an evident difference between the high-temperature situation, with only a few positive LCE, and the intermediate-temperature case, where there is a substantial agreement between \tilde{C}_ν and C_ν , for which all

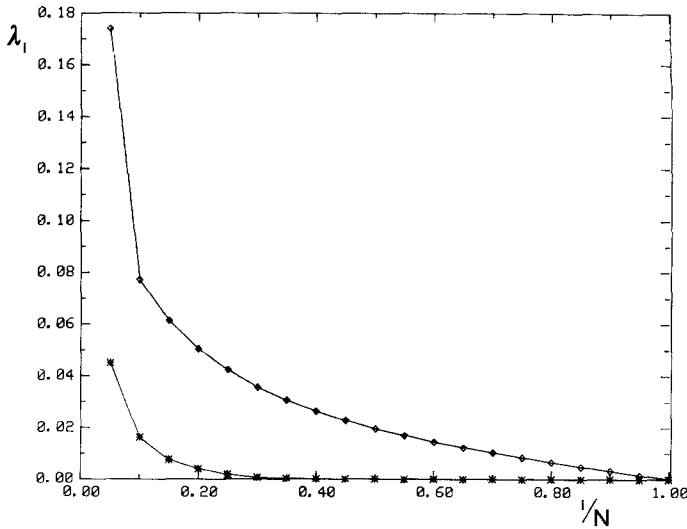


Fig. 7. LCE spectra. $\{\lambda_i\}$ is plotted versus i/N . (\diamond) $T/\epsilon = 1.0$, ($*$) $T/\epsilon = 50$. In both cases $N = 20$.

the LCE are positive. Moreover, we remark that λ_1 in Fig. 7 is significantly different from λ_1 reported in Fig. 3; this dependence on the initial conditions strengthens the above considerations about the phase space structure.

Similar results have been found with a smaller number of degrees of freedom.⁽¹⁵⁾

5. CONCLUSIONS

Our analysis has shown that: (a) there are situations in which the chaoticity of the system does not play a crucial role in the ergodicity of “relevant” physical quantities; (b) on the other hand, the exactly opposite situation can show up where the naive idea that chaoticity implies ergodicity fails. Although this framework could seem inconclusive, we suggest that from a physical point of view the situation is much more reasonable than one might think. In this respect the main suggestion of our analysis is that there exists a “hierarchy” of chaoticity levels corresponding to ergodicity for different classes of observables. For instance, in the FPU model the potential energy is always ergodic, slight deviations are found for specific heat, while the same system is extremely sensitive with respect to equipartition properties analyzed in the Fourier space. In the case of rotators we observe that, for potential energy, deviations appear only at high temperature, while specific heat begins to show a much stronger disagreement at lower temperature. In addition, one could think that the failure of equipartition at low temperature could be detected experimentally in real physical systems; in fact, the usual way of measuring the specific heat in solids at low temperatures is by means of calorimetric techniques, i.e., some energy input is produced in the system under investigation (for instance, by electromagnetic interactions) and then the temperature increase is measured; this method assumes that the energy input is quickly thermalized, while this might not be the case at very low temperatures.

As a final remark, we recall a simple example of how the observation time scale can affect the computation of ensemble averages. This is the case of the specific heat of the hydrogen molecule H_2 as reported by Ma.⁽¹⁶⁾ To compute the partition function for the H_2 molecule, the rotational energy and nuclear spin energy contributions are considered. The two different possibilities of parallel and antiparallel nuclear spins must be taken into account with their relative statistical weights. Then an important discrepancy is found at low temperatures between experimental results and theoretical predictions. The reason is that, during usual observation times, the nuclear spin of H_2 remains unchanged because of the very weak interactions with the electrons, of the weak interaction of the spins between

themselves, and of the negligible effect of the collisions; in other words, there is not statistical equilibrium. Thus, the correct calculation must take into account the effective number of molecules that are initially in the $s = 0$ and $s = 1$ states and consider them as invariant quantities.

APPENDIX A

A brief sketch of the definitions used for Liapunov exponents is reported here. Let the Hamilton equations of motion be written as

$$\dot{\mathbf{x}} = \mathbf{f}(\mathbf{x}) \tag{A.1}$$

where $\mathbf{x} = (q_1 \cdots q_N, p_1 \cdots p_N)$ and $f_i = \partial H / \partial x_{i+N}$ for $i = 1, \dots, N$, while $f_i = -\partial H / \partial x_{i-N}$ for $i = N + 1, \dots, 2N$. Then we define a vector \mathbf{J} in tangent space whose evolution is given by

$$\dot{J}_i = \sum_{k=1}^{2N} \frac{\partial f_i}{\partial x_k} J_k \tag{A.2}$$

where the derivatives are computed along the trajectory given by (A.1). The maximal Liapunov characteristic exponent λ_1 is defined as

$$\lambda_1 = \lim_{t \rightarrow \infty} \frac{1}{t} \ln \frac{\|\mathbf{J}(t)\|}{\|\mathbf{J}(0)\|} \tag{A.3}$$

and is computed with a standard method.⁽¹⁴⁾ To evaluate the complete spectrum of LCE an approach based on the expansion rates of p -dimensional subspaces⁽¹⁴⁾

$$\chi_p = \lim_{t \rightarrow \infty} \frac{1}{t} \ln \|\mathbf{J}^{(1)}(t) \times \mathbf{J}^{(2)}(t) \times \cdots \times \mathbf{J}^{(p)}(t)\| \tag{A.4}$$

is applied, where the $\mathbf{J}^{(k)}(t)$ evolve according to Eq. (A.2) and $\mathbf{J}^{(k)}(0)$ are orthonormal vectors with unitary norm. The Liapunov exponents are then given by

$$\sum_{i=1}^p \lambda_i = \chi_p \tag{A.5}$$

providing a basis for defining a numerical algorithm. In fact, a randomly chosen orthonormal basis in tangent space is made to evolve in time. The Gram-Schmidt orthogonalization procedure is then applied at fixed time intervals. This allows the evaluation of partial expansion rates and, at the same time, keeps the angles among the $\mathbf{J}^{(k)}(t)$ from becoming too small.

We remark that because of the symplectic structure of the Hamilton equations one has $\lambda_i = -\lambda_{2N-i+1}$; therefore one computes only the N non-negative LCE (i.e., $i \leq N$).

APPENDIX B. ENSEMBLE AVERAGES

Let us now compute the partition function for the FPU model whose Hamiltonian is given by Eq. (2).

The corresponding partition function is defined by the Gibbs measure as

$$Z_N = \int_{-\infty}^{\infty} \prod_{i=1}^N dp_i \exp\left(-\beta \sum_{i=1}^N \frac{1}{2} p_i^2\right) \times \int_{-\infty}^{\infty} \prod_{i=1}^N dq_i \exp\left\{-\beta \sum_{i=1}^N \left[\frac{1}{2} (q_{i+1} - q_i)^2 + \frac{1}{4} \lambda (q_{i+1} - q_i)^4\right]\right\} \quad (\text{B.1})$$

We make this calculation with free boundary conditions. The integration over the p_i is trivially done and gives a factor $(\pi/\beta)^{N/2}$, where $\beta = 1/k_B T$.

To calculate the configurational integral, we perform the following coordinate transformation:

$$\begin{aligned} \varphi_1 &= q_2 - q_1 \\ &\vdots \\ \varphi_{N-1} &= q_N - q_{N-1} \\ \varphi_N &= \bar{q} - q_N \\ \bar{\varphi} &= \bar{q} \end{aligned} \quad (\text{B.2})$$

where $\bar{\varphi}$ and \bar{q} are not true coordinates, but are parameters. It is easily verified that the Jacobian determinant of this transformation is nonsingular

$$\det \left[\frac{\partial(\varphi_1 \cdots \varphi_N \bar{\varphi})}{\partial(q_1 \cdots q_N \bar{q})} \right] = 1 \quad (\text{B.3})$$

The existence of the thermodynamic limit for this variable transformation is easily verified by looking at the contribution of the coordinate $\bar{\varphi}$ to the free energy. Thus, we can write

$$\begin{aligned} Z_N &= \left(\frac{\pi}{\beta}\right)^{N/2} \int_{-\infty}^{\infty} \prod_{i=1}^N d\varphi_i \exp\left[-\beta \sum_{i=1}^N \left(\frac{1}{2} \varphi_i^2 + \frac{1}{4} \lambda \varphi_i^4\right)\right] \\ &= \left(\frac{\pi}{\beta}\right)^{N/2} \left\{ \Gamma\left(\frac{1}{2}\right) \left(\frac{\beta \lambda}{2}\right)^{-1/4} \exp\left(\frac{\beta}{8\lambda}\right) D_{-1/2} \left[\left(\frac{\beta}{2\lambda}\right)^{1/2}\right] \right\}^N f(\bar{\varphi}) \quad (\text{B.4}) \end{aligned}$$

where Γ is the Euler gamma function and $D_{-1/2}$ is a parabolic cylinder function.

The free energy is then given by $F_N = -(1/N\beta) \log Z_N$ (we take $k_B = 1$),

$$F_N = -\frac{1}{2} T \ln \pi T - T \ln \Gamma\left(\frac{1}{2}\right) + \frac{1}{4} T \ln\left(\frac{\lambda}{2T}\right) - T \ln D_{-1/2}\left[\left(\frac{1}{2\lambda T}\right)^{1/2}\right] - \frac{1}{8\lambda} + O\left(\frac{1}{N}\right) \tag{B.5}$$

where the vanishing contribution $O(1/N)$, as N is increased, comes from $f(\bar{\varphi})$.

The specific heat C_V (at constant volume, as we deal with a constant-length, one-dimensional solid) is obtained as

$$C_V = -T(\partial^2 F / \partial T^2)$$

or, more explicitly,

$$C_V = \frac{3}{4} + 2T \frac{(d/dT) D_{-1/2}(\theta)}{D_{-1/2}(\theta)} + T^2 \frac{d}{dT} \left[\frac{(d/dT) D_{-1/2}(\theta)}{D_{-1/2}(\theta)} \right] \tag{B.6}$$

with $\theta = (1/2\lambda T)^{1/2}$, which can be reduced, with tedious but simple algebra, to

$$C_V = \frac{1}{2} + \frac{1}{2^8 \lambda T^2} \left\{ 2 + \frac{I_{-9/4}(\tau) - I_{9/4}(\tau) + I_{7/4}(\tau) - I_{-7/4}(\tau)}{I_{-1/4}(\tau) - I_{1/4}(\tau)} - \frac{[I_{-5/4}(\tau) - I_{5/4}(\tau) + I_{3/4}(\tau) - I_{-3/4}(\tau)]^2}{[I_{-1/4}(\tau) - I_{1/4}(\tau)]^2} \right\} \tag{B.7}$$

where $I_\nu(\tau)$ is a modified Bessel function and $\tau = 1/8\lambda T$.

For sufficiently low temperatures, θ and τ become large, and therefore we can use the asymptotic expansion

$$D_{-1/2}(x) \sim e^{-x^2/4} x^{-1/2} \left(1 - \frac{3}{8x^2} + \dots \right) \tag{B.8}$$

which, introduced in the above expression for C_V , yields

$$C_V \simeq \frac{3}{4} + \frac{1/2 - (15/8) \lambda T}{1 - (3/4) \lambda T} - \frac{1}{4} \frac{1}{1 - (3/4) \lambda T} + \frac{(3/16) \lambda T - (45/64) \lambda T^2}{(1 - (3/4) \lambda T)^2} \tag{B.9}$$

having the right limiting value $C_V = 1$ when λ , the nonlinear coupling constant, or T is set equal to zero.

The ensemble average of the specific potential energy can be calculated by means of

$$\langle \mathcal{U} \rangle = -\frac{1}{N} (Z_N^c)^{-1} \frac{\partial Z_N^c}{\partial \beta} \quad (\text{B.10})$$

where Z_N^c is the configurational part of the partition function. In the high- β limit (low temperature), we can use the asymptotic expansion of Eq. (B.9) for the parabolic cylinder functions; thus,

$$\begin{aligned} \langle \mathcal{U} \rangle \simeq & -\frac{1}{N} \frac{\partial}{\partial \beta} \left\{ \left(\frac{\beta}{2} \right)^{-N/2} \left(1 - \frac{3\lambda}{4\beta} \right)^N \right\} \\ & \times \left[\left(\frac{\beta}{2} \right)^{-N/2} \left(1 - \frac{3\lambda}{4\beta} \right)^N \right]^{-1} \end{aligned} \quad (\text{B.11})$$

and then

$$\langle \mathcal{U} \rangle \simeq \frac{1}{2} T - \frac{(3/4)\lambda T^2}{1 - (3/4)\lambda T}$$

which is useful essentially at low temperatures.

At high temperatures we use the full analytic result, which reads

$$\begin{aligned} \langle \mathcal{U} \rangle = & (Z_1^c)^{-1} \Gamma\left(\frac{1}{2}\right) e^{\beta/8\lambda} \left(\left[\frac{1}{4} \left(\frac{\lambda}{2} \right)^{-1/4} \beta^{-5/4} - \frac{1}{8\lambda} \left(\frac{\beta\lambda}{2} \right)^{-1/4} \right] D_{-1/2} \left[\left(\frac{\beta}{2\lambda} \right)^{1/2} \right] \right. \\ & + \frac{1}{8\lambda} \left(\frac{\beta\lambda}{2} \right)^{-1/4} \left(\frac{\beta}{2\lambda} \right)^{-1/2} \left\{ \left(\frac{\beta}{2\lambda} \right)^{1/2} D_{-1/2} \left[\left(\frac{\beta}{2\lambda} \right)^{1/2} \right] \right. \\ & \left. \left. + D_{-3/2} \left[\left(\frac{\beta}{2\lambda} \right)^{1/2} \right] \right\} \right) \end{aligned} \quad (\text{B.12})$$

where Z_1^c is given by

$$Z_1^c = \Gamma\left(\frac{1}{2}\right) \left(\frac{\beta\lambda}{2} \right)^{-1/4} e^{\beta/8\lambda} D_{-1/2} \left[\left(\frac{\beta}{2\lambda} \right)^{1/2} \right]$$

Now we perform the same calculation for a weakly coupled chain of rotators described by the Hamiltonian given in Eq. (3). Its partition function is

$$\begin{aligned}
 Z_N = & \int_{-\infty}^{\infty} \prod_{i=1}^N dp_i \exp \left(-\beta \sum_{i=1}^N \frac{1}{2} p_i^2 \right) \\
 & \times \int_{-\pi}^{\pi} \prod_{i=1}^N dq_i \exp \left\{ -\beta \varepsilon \sum_{i=1}^N [1 - \cos(q_{i+1} - q_i)] \right\} \quad (\text{B.13})
 \end{aligned}$$

where, again, $\beta = 1/T$, $k_B = 1$.

We consider again free boundary conditions.

The first integral is trivially computed and gives the same contribution $(\pi/\beta)^{N/2}$.

To evaluate the contribution of the configurational integral, the same transformation of variables has to be made:

$$\begin{aligned}
 \omega_1 &= q_2 - q_1 \\
 &\vdots \\
 \omega_{N-1} &= q_N - q_{N-1} \\
 \omega_N &= \bar{q} - q_N \\
 \bar{\omega} &= \bar{q}
 \end{aligned} \quad (\text{B.14})$$

and again the Jacobian determinant is equal to 1; the ω_i vary in the interval $[0, 2\pi]$.

Consequently, we get

$$\begin{aligned}
 Z_N &= \left(\frac{\pi}{\beta}\right)^{N/2} \int_0^{2\pi} \prod_{i=1}^N d\omega_i \exp \left(\beta \sum_{i=1}^N \varepsilon \cos \omega_i \right) \exp(-\beta \varepsilon N) \\
 &= \left(\frac{\pi}{\beta}\right)^{N/2} \exp(-\beta \varepsilon N) [I_0(\varepsilon \beta)]^N g(\bar{\omega}) (2\pi)^N \quad (\text{B.15})
 \end{aligned}$$

where $I_0(x)$ is a modified Bessel function and $g(\bar{\omega})$ is a function of the parameter $\bar{\omega}$.

Hence we get the following expression for the free energy:

$$F_N = -T \left[\frac{1}{2} \ln \pi + \frac{1}{2} \ln T + \ln I_0 \left(\frac{\varepsilon}{T} \right) \right] + \varepsilon - T \ln 2\pi + O \left(\frac{1}{N} \right) \quad (\text{B.16})$$

and finally we get for the specific heat

$$C_V = \frac{1}{2} + \beta^2 \left\{ 1 - \frac{1}{\beta} \frac{I_1(\varepsilon \beta)}{I_0(\varepsilon \beta)} - \left[\frac{I_1(\varepsilon \beta)}{I_0(\varepsilon \beta)} \right]^2 \right\} \quad (\text{B.17})$$

which is easily evaluated numerically.

Another quantity that we can straightforwardly compute is the average specific potential energy, given by

$$\langle \mathcal{U} \rangle = -\frac{1}{N} \frac{\varepsilon}{\beta} Z_N^{-1} \frac{\partial Z_N}{\partial \varepsilon} \quad (\text{B18})$$

from which we get

$$\langle \mathcal{U} \rangle = \varepsilon \left[1 - \frac{I_1(\varepsilon\beta)}{I_0(\varepsilon\beta)} \right] \quad (\text{B19})$$

We would like to make the reader aware of an unpleasant surprise that we had in using three different and widespread mathematical libraries while computing $I_\nu(x)$ functions. When the arguments are of the order of few units, the results are completely wrong, but no warning about argument limitations is reported in the handbooks.

ACKNOWLEDGMENTS

We thank C. Agnes and M. Rasetti for discussions, comments, and their interest in this work. It is a pleasure to thank R. Lima for criticism, discussions, and suggestions.

The computer simulations reported here have been financed by the Italian Istituto Nazionale di Fisica Nucleare. This work was completed at the Institute for Scientific Interchange in Torino, whose kind hospitality is warmly acknowledged.

REFERENCES

1. R. C. Tolman, *The Principles of Statistical Mechanics* (Oxford University Press, 1938).
2. A. I. Khinchin, *Mathematical Foundations of Statistical Mechanics* (Dover New York, 1949).
3. C. Truesdell, in *Ergodic Theory, Proceedings of the International School of Physics 'Enrico Fermi'*, P. Caldirola, ed. (Varenna, 1960), p. 21.
4. F. M. Izraïlev and B. V. Chirikov, *Sov. Phys. Doklady* **11**:30 (1966).
5. P. Bocchieri, A. Scotti, B. Bearzi, and A. Loinger, *Phys. Rev. A* **2**:2013 (1970); M. Casartelli, G. Casati, E. Diana, L. Galgani, and A. Scotti, *Theor. Math. Phys.* **29**:205 (1976) (in Russian); M. Casartelli, E. Diana, L. Galgani, and A. Scotti, *Phys. Rev. A* **13**:1921 (1976).
6. R. Livi, M. Pettini, S. Ruffo, M. Sparpaglione, and A. Vulpiani, *Phys. Rev.* **28**:3544 (1983); *Phys. Rev. A* **31**:1039 (1985); R. Livi, M. Pettini, S. Ruffo, and A. Vulpiani, *Phys. Rev. A* **31**:2740 (1985).
7. J. Bellissard and M. Vittot, Marseille preprint CPT-MARSEILLE (1985), to appear in *Ergodic Theory and Dynamical Systems*; J. Fröhlich, T. Spencer, and C. E. Wayne, *J. Stat. Phys.* **42**:247 (1986).

8. E. Schrödinger, *Ann. Physik* **44**:916 (1914); H. Wergeland, in *Irreversibility in Many-Body Problems*, J. Biel and J. Rae, eds. (Plenum Press, New York, 1972), p. 105; G. Casati, *Found. Phys.* **16**:51 (1986).
9. F. Mokross and H. Büttner, *J. Phys. C* **16**:4539 (1983); G. Casati, J. Ford, F. Vivaldi, and W. M. Visscher, *Phys. Rev. Lett.* **52**:1861 (1984).
10. M. Casartelli, *Phys. Rev. A* **19**:1741 (1979); M. C. Carotta, C. Ferrario, G. Lo Vecchio, B. Carazza, and L. Galgani, *Phys. Lett.* **57A**:399 (1976); R. W. Hall and B. J. Berne, *J. Chem. Phys.* **81**:3641 (1984).
11. E. Fermi, J. Pasta, and S. Ulam, in *Collected papers of E. Fermi*, (University of Chicago, Chicago, 1965), Vol. 2, p. 978.
12. L. Verlet, *Phys. Rev.* **159**:89 (1967).
13. R. Livi, A. Politi, and S. Ruffo, *J. Phys. A: Math. Gen.* **19**:2033 (1986).
14. G. Benettin, L. Galgani, and J. M. Strelcyn, *Phys. Rev. A* **14**:2338 (1976); G. Benettin, L. Galgani, A. Giorgilli, and J. M. Strelcyn, *Meccanica* **15**:9 (1980); **15**:21 (1980).
15. G. Benettin, L. Galgani, and A. Giorgilli, *Nuovo Cimento B* **89**:103 (1985).
16. S. K. Ma, *Statistical Mechanics* (World Scientific, Singapore, 1985), p. 142.